Analysis of Sampling Grids for Spherical Near-field Antenna Measurements

R. Cornelius and D. Heberling
Institute of High Frequency Technology, RWTH Aachen University, Germany

Abstract— Modern spherical near-field to far-field transformation algorithms, in contrast to Fourier based ones, offer arbitrary sampling grids without inherent oversampling. This raises the question how the measurement samples should be distributed on the sphere. In this paper different sampling grids for spherical near-field antenna measurements are presented and evaluated. It is shown that the spherical transformation problem is in general well-conditioned and can be solved accurately. Measurement results emphasize the possible measurement time reduction due to the reduction of oversampling. However, positioning hardware has to be included in the analysis, because complex measurement trajectories might increase the measurement time.

1. INTRODUCTION

Spherical near-field antenna measurement is a popular, well-known and accurate method to characterize an antenna under test (AUT). The electromagnetic field is measured on a closed surface around the antenna and transformed to the far-field by a near-field to far-field transformation. A commonly used transformation algorithm first calculates a spherical mode spectrum using Fourier transforms [1]. From this mode spectrum the far-field is derived. Due to the Fourier transform the transformation algorithm is very fast and efficient but requires equiangular sampling in spherical coordinates which causes oversampling. In order to improve the measurement speed more efficient sampling grids may be used at the expense of different and/or more complex transformation algorithms. Reformulating the transmission formula in [1] in matrix form as used for truncation error reduction in [2] is a very simple and straightforward approach which will be used in this paper. Alternatively, algorithms not restricted to equiangular sampling [3, 4] could be used. Furthermore, near-field interpolation methods could be utilized to determine the near-field on an equiangular grid [5]. Besides the larger sampling flexibility new algorithms provide additional features like higher order probe correction, the possibility of different measurement distances and position correction. Due to the technical progress in computer technology the transformation time is usually negligible compared to the measurement time and therefore a less important factor. Although new algorithms have been successfully tested by simulations and measurements [3, 4, 6], a comprehensive investigation of different sampling grids is still missing. So far only little attention has been paid to the minimal number of required near-field samples and their distribution over the sphere. This distribution is also a very important factor for the measurement time due to different capabilities of different positioning systems (e.g., roll-over-azimuth, robot arm). In this paper we will present different sampling grids and besides the location of the sampling points the polarization will be investigated. The near-field to far-field transformation algorithm used is based on calculation of the spherical modes by matrix inversion. Therefore the condition number of the grids will be evaluated and compared. Simulations and measurements will be performed for all grids. Finally the required relative measurement time and accuracy will be analyzed for the different sampling grids. It will be highlighted that the measurement speed can be increased compared to equiangular sampling.

2. NF-FF TRANSFORMATION USING MATRIX INVERSION

The well-known spherical near-field transmission formula [1]

$$w(A,\chi,\theta,\phi)=\sum_{\substack{smn\\ \mu}} Q_{smn}e^{im\phi}d^{n}_{\mu m}(\theta)e^{i\mu\chi}P_{s\mu n}(kA) \tag{1}$$

can be directly interpreted as a linear equation system

$$\mathbf{w}=\Psi\mathbf{Q} \tag{2}$$

where $\mathbf{w}$ is the measured signal, Q_{smn} are the spherical mode coefficients, $e^{im\phi}d^{n}_{\mu m}(\theta)e^{i\mu\chi}$ represents the spherical mode rotation and $P_{s\mu n}$ are the probe coefficients. Spherical modes are orthogonal solutions of Maxwell's equations in spherical coordinates. Their complex amplitudes are denoted as Q_{smn} and have three indices: degree n, order $m \leq n$ and $s \in [1, 2]$ associated to the field components of TE- and TM-waves. In antenna measurements the modes are band limited in $m \in [1, M]$ and $n \in [1, N]$ according to:

$$M \leq N = kr_0 + n_1 \tag{3}$$

k is the wavenumber, r_0 is the radius of a sphere containing the antenna and n_1 is a constant which influences the accuracy (usually 10, [1]). Thus the highest mode excited by an AUT is limited by its size in relation to frequency. Higher order modes are highly attenuated and do not contribute significantly to the far-field characteristic. The total number of modes ($M = N$), equal to the number of unknowns, can be calculated from its band limitation by

$$\#_{Modes} = P_{\min} = 2N(N+2) = 2N^2 + 4N \tag{4}$$

The linear equation system (2) can be solved with different methods as for example least squares [6] and does in general not require any specific sampling grid. Methods based on matrix inversion require of course more computational power but are affordable for antenna measurement applications with several thousands of measurement points.

3. POINT DISTRIBUTION ON SPHERE

In general, infinitely many possibilities exist to distribute P points on a sphere and as stated above no specific sampling criterion has to be fulfilled. However, in antenna measurement applications covering the whole sphere is required in order to avoid truncation errors [2]. Therefore the measurement points need to cover the whole sphere. Equal distribution is an intuitive choice but not compulsory. The investigated schemes are:

3.1. Equiangular

The required equiangular sampling steps are calculated from the band limitation by

$$\Delta\theta = \frac{2\pi}{(2N+1)}; \quad \Delta\varphi = \frac{2\pi}{(2M+1)} \leq \frac{2\pi}{(2N+1)}; \quad \chi = \left[0, \frac{\pi}{2}\right]; \tag{5}$$

$$P = P_\theta P_\varphi P_\chi = (N+1)(2N+1) \cdot 2 = 4N^2 + 6N + 2 \tag{6}$$

The samples are concentrated near the poles and the sphere is therefore highly oversampled (roughly by factor of 2).

3.2. Thinned Equiangular

A sampling strategy to reduce the oversampling at the poles is the reduction of measurement points in φ depending on the value θ taking into account the fact that the latitude circles have different radii ($\propto \sin(\theta)$).

$$\Delta\theta = \frac{2\pi}{(2N+1)}; \quad \Delta\varphi = \frac{2\pi}{\lceil (2M+1)\sin(\theta) \rceil} \leq \frac{2\pi}{\lceil (2N+1)\sin(\theta) \rceil}; \quad \chi = \left[0, \frac{\pi}{2}\right] \tag{7}$$

3.3. Platonic

Platonic solids are an exact solution to the distribution problem for $P = (4, 6, 8, 12, 20)$. If more samples are required tessellation of the platonic solid can be used but is restricted to fixed numbers which makes it very inflexible. For this reason they are not very useful in measurement practice but are included in the analysis for reference.

3.4. Spiral

Spiral scanning schemes on the sphere are appropriate to distribute points equally on the sphere [6, 7]. The spiral scanning scheme used for our analysis is based on [7], where the slope is fixed:

$$\varphi = \alpha\theta \tag{8}$$

The slope is determined so that the distance between two spiral lines is equal to the distance Δs between two neighboring points equally placed along the spiral path.

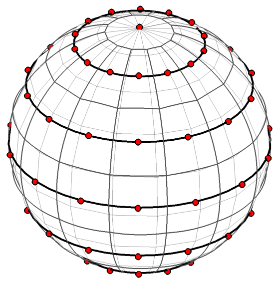

Figure 1: Equiangular sampling.

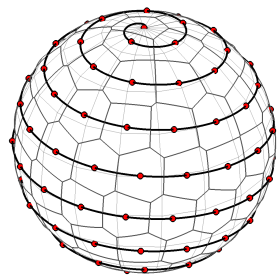

Figure 2: Spiral sampling.

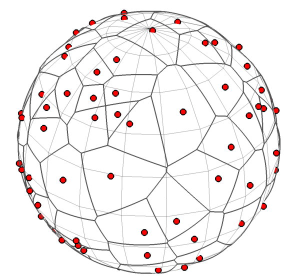

Figure 3: Random sampling.

Table 1: Sampling point distribution analysis.

Sampling	P	ΔA_{area}	$\Delta d_{\text{distance}}$
Equiangular	2664	39.0%	25.9%
Thinned equiangular	2698	0.4%	1.7%
Platonic (Dodecahedron)	1922	2.0%	1.0%
Platonic (Icosahedron)	2562	6.4%	2.9%
Spiral	2664	0.3%	1.2%
Random	2664	41.5%	23.5%

3.5. Random

Although deterministic sampling schemes provide advantageous features as deterministic uncertainty analysis and well defined trajectories, random point distributions are also suitable. The random sampling scheme is included in the analysis to emphasize the bandwidth of sampling possibilities.

3.6. Geometric Comparison of Sampling Grids

Figure 1 to Figure 3 show selected sampling grids including Voronoi cells for a low number of sampling points. The different sampling grids are evaluated by two measures

1. Mean of the relative Voronoi cell area difference to the mean cell area (ΔA_{area}).
2. Mean of the relative distance variation of neighboring samples ($\Delta d_{\text{distance}}$).

which are shown in Table 1. As expected the variation of the Voronoi cell area is very large for equiangular sampling. The variations are reduced for all other deterministic sampling methods which perform very well. It is important to note that the number of samples $P \geq P_{\min}$ can only be defined arbitrarily for spiral and random sampling. Furthermore, random sampling does also not generate well distributed points.

4. POLARIZATION ANALYSIS

So far only the location of the sampling point has been considered. The polarization of the probe at each sampling position is an additional parameter which has to be included in the analysis. Three major possibilities will be considered for further analysis:

1. Randomly chosen polarization ($\chi \in [0, 2\pi]$) at each sampling point.
2. Two orthogonal polarizations at each sampling point.
3. Randomly chosen fixed polarization ($\chi = 0$ or $\chi = \frac{\pi}{2}$) at each sampling point.

Measurements with only one fixed polarization are, as expected, not possible and due to missing information the matrix always gets singular. To study different selections of the polarization, the condition number of the matrix Ψ is calculated for various oversampling ratios. Figure 4 shows the condition number for polarization case 1. Equiangular and thinned equiangular are well-conditioned but always oversampled. A reduction of the oversampling is not possible and leads to singular matrices - these points are excluded from the plot. For spiral and random sampling the oversampling can be reduced by the cost of a worse condition number. However, even for the determined system the matrix is not singular. The behavior changes slightly if at each point

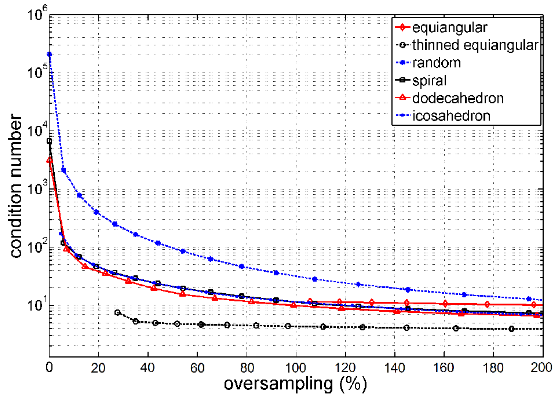

Figure 4: Condition number for case 1.

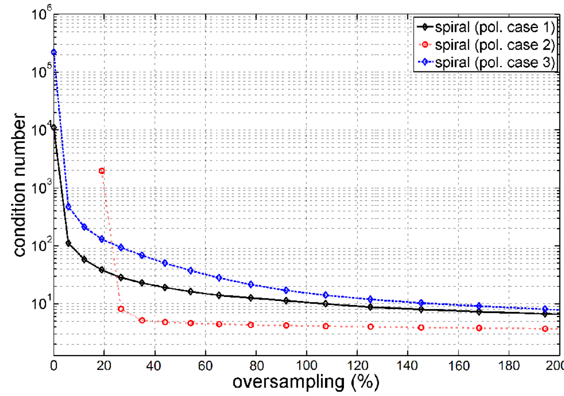

Figure 5: Condition number for spiral sampling.

Table 2: Simulation mode differences compared to FT based results.

Sampling	P	Over.	cond.	Noiseless		Noisy (SNR = 70 dB)	
				ΔQ_{mean}	$\Delta Q_{\max}$	ΔQ_{mean}	$\Delta Q_{\max}$
Equiangular	2660	108%	9	−318 dB	−291 dB	−82.1 dB	−72.5 dB
Thinned equiangular	1588	27%	6	−319 dB	−296 dB	−81.1 dB	−70.7 dB
Platonic (Dodecahedron)	1922	54%	15	−316 dB	−295 dB	−79.5 dB	−70.0 dB
Platonic (Icosahedron)	1284	3%	173	−314 dB	−290 dB	−76.4 dB	−55.8 dB
Spiral	1498	20%	35	−314 dB	−293 dB	−75.0 dB	−65.8 dB
Random	1498	20%	160	−306 dB	−294 dB	−65.2 dB	−54.8 dB

two orthogonal polarizations (case 2) or randomly chosen fixed polarizations (case 3, Figure 5) are measured. For spiral scanning the matrix gets singular for case 2 if the oversampling ratio tends towards zero. This linear dependencies are assumed to result from the fact that the number of locations (θ, φ) is halved compared to the other cases in order to keep the total number of samples constant. Further analysis showed that the condition number increases slightly with the number of unknowns. In conclusion, the polarization measurement method is not a crucial parameter as long as the condition number, which can be calculated in advance, is still acceptable. Therefore it can be selected mainly according to system possibilities.

5. SIMULATION RESULTS

A simulated 64 element dipole array is used to investigate the effect on the spherical mode calculation. The electric near-field of the dipole array is simulated for the different sampling grids. Next, the absolute linear differences in the mode spectrum are calculated for evaluation.

$$\Delta Q = |Q_{FT} - Q_{iSampling}| \tag{9}$$

Although the matrix solution of the transmission formula does not differ significantly from the Fourier transform (FT) based solution [6], the calculated modes are compared to the FT based algorithm, because this is a well accepted method. The results are summarized in Table 2 and show that in the noiseless and noisy case all sampling grids are suitable to achieve accurate results compared to the Fourier transform algorithm. The differences for equiangular sampling are the differences between the Fourier transform and least squares algorithm. Due to the higher condition number, icosahedron and random sampling have larger errors.

6. MEASUREMENT RESULTS

Measurements in the spherical near-field measurement chamber of the Institute of High Frequency Technology were performed with an double ridged horn SAS-571 from AH-System as test object. The measurement results are summarized in Table 3. The relative measurement time t_{rel} is improved by one third with thinned equiangular and spiral scanning compared to equiangular. However platonic and random sampling takes more time, even when having less samples, because of sub-optimal measurement trajectories. Optimization of these is a complex task and is out of the

Table 3: Measurement mode differences compared to FT based results.

Sampling	P	t_{rel}	t_{point}	cond.	ΔQ_{mean}	$\Delta Q_{\max}$
Equiangular LS (same data as FT)	2400	100%	5.0 s	9	−103.9 dB	−68.8 dB
Equiangular LS (rep. meas.)	2400	100%	5.0 s	9	−71.2 dB	−38.3 dB
Thinned equiangular	1464	66%	5.5 s	6	−74.2 dB	−42.0 dB
Platonic (Dodecahedron)	1922	228%	14.4 s	13	−68.0 dB	−40.4 dB
Platonic (Icosahedron)	1284	142%	13.5 s	6	−70.9 dB	−41.8 dB
Spiral	1380	63%	5.6 s	29	−66.3 dB	−43.4 dB
Random	1380	136%	12.2 s	146	−59.4 dB	−36.1 dB

scope of this paper. For equiangular sampling the difference between both algorithm (first row) and two successive measurements (reproducibility, second row) are shown. According to these values all measurement grids perform good and the mean difference for thinned equiangular is the smallest. Higher condition numbers increase especially the maximum error and are a good uncertainty parameter.

7. CONCLUSION

In this paper a set of sampling schemes for spherical near-field antenna measurements was investigated. The main advantage of non-equiangular sampling grids is the reduction of oversampling. It was shown by simulation that the new sampling grids provide a well-conditioned linear equation system which can be solved accurately. Furthermore measurements were performed to investigate the realized accuracy and measurement speed. The main result is that the total measurement time can be reduced, but depends on the positioning system. In addition, it has been found that the transformation error is closely linked to the condition number and is thus well suited for uncertainty estimation.

REFERENCES

1. Hansen, J. E., *Spherical Near-field Antenna Measurements*, Peter Peregrinus Ltd., United Kingdom, 1988.
2. Wittmann, R. C., C. F. Stubenrauch, and M. H. Francis, "Spherical scanning measurements using truncated data sets," *Proceedings of the 24th AMTA Annual Meeting & Symposium*, Nov. 2002.
3. Sarkar, T. and A. Taaghol, "Near-field to near/far-field transformation for arbitrary near-field geometry utilizing an equivalent current and MoM," *IEEE Trans. Antennas Propag.*, Vol. 47, No. 3, 566–573, 1999.
4. Schmidt, C., M. Leibfritz, and T. Eibert, "Fully probe-corrected nearfield far-field transformation employing plane wave expansion and diagonal translation operators," *IEEE Trans. Antennas Propag.*, Vol. 56, No. 3, 737–746, 2008.
5. Bucci, O. M., C. Gennarelli, and F. D'Agostino, "A new and efficient NF-FF transformation with spherical spiral scanning," *Proceedings of IEEE Antennas and Propagation Society International Symposium*, Jul. 2001.
6. Cornelius, R., M. Dirix, H. Shakhtour, and D. Heberling, "Investigation of different matrix solver for spherical near-field to far-field transformation," *Proceedings of the 9th European Conference on Antennas and Propagation (EuCAP 2015)*, Apr. 2015.
7. Saff, E. and A. Kuijlaars, "Distributing many points on a sphere," *The Mathematical Intelligencer*, 1997.
8. Koay, C. G., "Analytically exact spiral scheme for generating uniformly distributed points on the unit sphere," *Journal of Computational Science*, 2011.